

Article

# Deterioration Process of Concrete Exposed to Internal Sulfate Attack

Weifeng Chen <sup>1,2</sup>, Bei Huang <sup>1,2,\*</sup>, Yuexue Yuan <sup>1,2</sup> and Min Deng <sup>1,2</sup>

<sup>1</sup> College of Materials Science and Engineering, Nanjing Tech University, Nanjing 211800, China; chenweifeng@njtech.edu.cn (W.C.); yxynjtech@126.com (Y.Y.); dengmin@njtech.edu.cn (M.D.)

<sup>2</sup> State Key Laboratory of Materials-Oriented Chemical Engineering, Nanjing 211800, China

\* Correspondence: bhnjtech@163.com; Tel.: +86-138-5160-2803

Received: 10 February 2020; Accepted: 13 March 2020; Published: 15 March 2020



**Abstract:** Damage to concrete structures with gypsum-contaminated aggregate occurs frequently. Aggregates in much of the southern part of China are contaminated with gypsum. Therefore, in this study, the effects of using different quantities of gypsum-contaminated aggregate on the expansion and compressive strength of concrete were investigated over a period of one year. Two groups of concrete were designed with the gypsum-contaminated aggregate containing different parts of fine and coarse aggregate, respectively. The SO<sub>3</sub> contents were 0%, 0.5%, 1%, 1.5%, 3%, 5%, and 7% by weight of aggregate. X-ray diffraction (XRD), thermogravimetry (TG), and differential scanning calorimetry (DSC) were used to analyze the change in mineral composition over time. The microstructure was also studied by scanning electron microscopy (SEM) and energy dispersive spectrometry (EDS). The results showed that significant expansion and great loss in compressive strength did not occur in concrete if the content of SO<sub>3</sub> lay below 1.5% and 3% in fine and coarse aggregates, respectively. The concentration of sulfate ions in concrete was not enough to form new a phase of gypsum. During the process of internal sulfate attack, the content of gypsum decreased and the content of ettringite increased. Ettringite was the main reason for the expansion damage of concrete. Additionally, the fracture mode of internal sulfate attack on concrete was the crack extension from gypsum to paste; finally, the aggregate separated from the paste.

**Keywords:** internal sulfate attack; concrete; gypsum; performance

## 1. Introduction

Sulfate attack on concrete is a key durability problem. Internal sulfate attack (ISA) on concrete is a reaction between sulfates present in the original mix of concrete and the calcium aluminate in cement and water, which can show signs of deterioration [1]. In the early stage of hydration, the gypsum reacts with tricalcium aluminate to form ettringite (AFt), which does not damage concrete. It is beneficial and leads to an increase in strength. However, the excess gypsum remains in the hardened concrete, and the gypsum will dissolve sulfate ions. The SO<sub>4</sub><sup>2-</sup> continues to react with the remaining tricalcium aluminate to form AFt, which is harmful to concrete [2]. The harmful AFt may cause a deleterious expansion and strength loss, since large stresses are generated in the hardened cement paste [3]. In the past 30 years, ISA damage due to aggregates with sulfate salts has been found in tunnels and dams in China [4], Middle Eastern countries [5], and some European countries [6]. A large number of engineering disasters have occurred because of the aggregate contained in sulfates. As a result, great economic losses as well as safety problems have arisen.

The mechanism of external sulfate attack (ESA) has been studied for many years. Sulfate is supplied by seawater, groundwater, and industrial wastewater. Sulfate ions react with ionic species of the pore solution to precipitate ettringite, gypsum, or thaumasite [7]. The major reaction product of ESA

is AFt. The formation of AFt results in expansion and cracking, spalling, and other damaging effects. There is a correlation between the  $C_3A$  content in Portland cement and the susceptibility of concrete to sulfate attack, and cements with limited  $C_3A$  content were introduced to the market. These cements are used in the concrete that is exposed to moderate and severe sulfate concentrations [8,9]. The sulfate ions react with portlandite to form gypsum. Even though gypsum formation is generally accepted to be harmful, the specific mechanism by which this occurs is not well established. It is widely accepted that gypsum formation only has a softening effect and causes mass and strength loss. However, Tian demonstrated that gypsum formation during sulfate attack may cause expansion [10]. The development of gypsum is influenced by the pH value and the concentration of sulfate ions. In sulfate solution, the minimum concentration of sulfate ions to form gypsum is 1400 mg/L, at a pH value equal to 12.4 [11]. Normally, gypsum is the first reaction product at a high sulfate ion concentration, especially  $SO_4^{2-} > 8000$  mg/L [12]. Thaumate is usually considered to be formed at a low temperature in the presence of carbonate [13]. The thaumate form of sulfate attack is different from ettringite formation because it is the C-S-H in hardened Portland cement that is targeted for the reaction and not the calcium aluminate hydrates. However, C-S-H is the primary binding agent in concrete [14].

Compared with the sulfate ions that penetrate into concrete by diffusion for ESA, there is a higher concentration of sulfate ions in concrete for ISA. The hazard is illustrated in the materials which cause higher tensile stress, leading to spalling and disruption of concrete structures [15]. For example, several highway tunnels in China were damaged seriously by ISA in the year after they were built. In order to prevent ISA, Chinese national standards have set the upper limit for the  $SO_3$  content in fine and coarse aggregates. It is stipulated in GB/T14684 and GB/T14685 that the  $SO_3$  content in fine and coarse aggregates shall not exceed 0.5% and 1%, respectively. Samarai proposed a 0.1% expansion as a safe margin for finding the allowable sulfate level [16]. According to Crammond, the allowable gypsum content in aggregates used in Portland cement mortars would not be much larger than 2.5% by weight of aggregate [17]. Because of the higher concentration of sulfate ions, the types of reaction products and the degradation process of ISA are important problems to be studied. In this paper, the expansion, strength loss, and formation process of reaction products of concrete with different amounts and particle sizes of gypsum-contaminated aggregate were investigated, and we aimed to discuss the feasibility of using gypseous rock as a concrete aggregate for highways in Shanxi province.

## 2. Research Significance

In this paper, the influences of the dosage of gypsum aggregate on the compressive strength and expansion performance of concrete were studied. The types of reaction products in the process of internal sulfate attack were also studied.

## 3. Materials and Mixes

### 3.1. Raw Materials

P-II 52.5 Portland cement conforming to Chinese National Standard GB175 was used in this study and its chemical composition is shown in Table 1. Two types of aggregate were used. One was gypseous aggregate, which was crushed into fine and coarse aggregate, from the WU YAN HE railway tunnel from Shanxi province to Shandong province. Another was normal aggregate with no gypsum; river sand was used as fine aggregate and limestone was used as coarse aggregate. The appearance of gypsum-contaminated aggregate is shown in Figure 1. The chemical compositions and XRD patterns of this aggregate are shown in Table 2 and Figure 2, respectively. The chemical compositions of white part (WP) are shown in Table 3. From analysis results, it was found that the WP of this rock was a mix of gypsum and anhydrite, and the rock matrix was dolomite.



Figure 1. Appearance of gypsum-contaminated aggregate.

Table 1. Chemical compositions of P-II 52.5 Portland cement.

SiO <sub>2</sub>	CaO	Al <sub>2</sub> O <sub>3</sub>	Fe <sub>2</sub> O <sub>3</sub>	MgO	Na <sub>2</sub> O	SO <sub>3</sub>
19.46	63.23	4.53	2.80	2.41	0.13	3.31

Table 2. Chemical compositions of gypsum-contaminated aggregate.

SiO <sub>2</sub>	CaO	Al <sub>2</sub> O <sub>3</sub>	Fe <sub>2</sub> O <sub>3</sub>	MgO	K <sub>2</sub> O	Na <sub>2</sub> O	SO <sub>3</sub>	LOI
15.83	17.21	6.71	4.64	11.59	2.87	0.26	18.03	21.08

Table 3. Chemical compositions of the white part (WP) in aggregate.

SiO <sub>2</sub>	CaO	Al <sub>2</sub> O <sub>3</sub>	MgO	Fe <sub>2</sub> O <sub>3</sub>	SO <sub>3</sub>	K <sub>2</sub> O	Na <sub>2</sub> O	TiO <sub>2</sub>	LOI
0.19	35.43	0.08	4.05	0.02	51.36	0.01	0.01	0.01	12.79

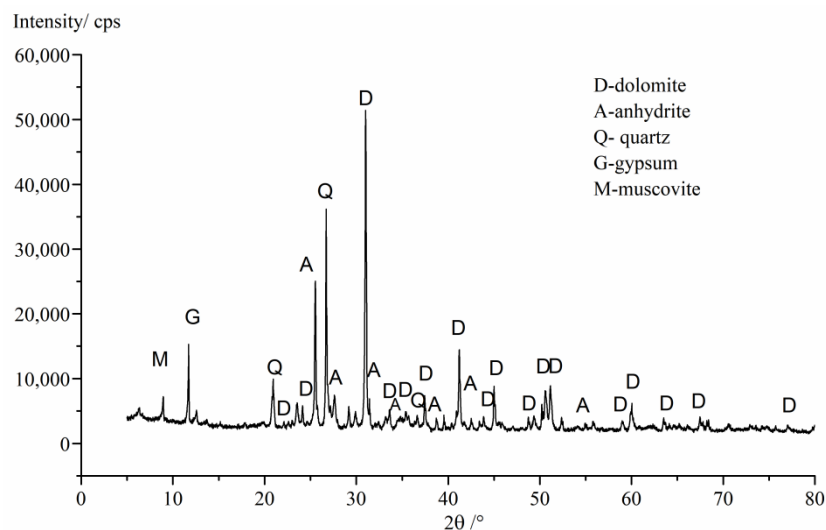


Figure 2. XRD patterns of gypsum-contaminated aggregates.

### 3.2. Mix Proportion

In our experimental program, there were two types of concrete specimen: 100 mm by 100 mm by 100 mm and 75 mm by 75 mm by 280 mm. They were demolded a day after casting and cured in water at 20 ± 2 °C. The cube samples were used to determine the compressive strength of the concrete with different amounts and sizes of gypsum. The prism specimens were used for the ultrasonic and expansion test of concrete at different ages.

The gypsum-contaminated aggregate was crushed into gypsum sand (<4.75 mm) and gypsum stone (5–20 mm). Part of the normal fine and coarse aggregate was replaced with gypsum-contaminated aggregate in the mixture of concrete, to get five levels of SO<sub>3</sub> content (0, 0.5%, 1.0%, 1.5%, 3.0%, 5.0%, and 7% by weight of aggregate) in the concrete. The grain size curves of fine and coarse aggregates are shown in Figure 3. The mix design of concretes is shown in Table 4.

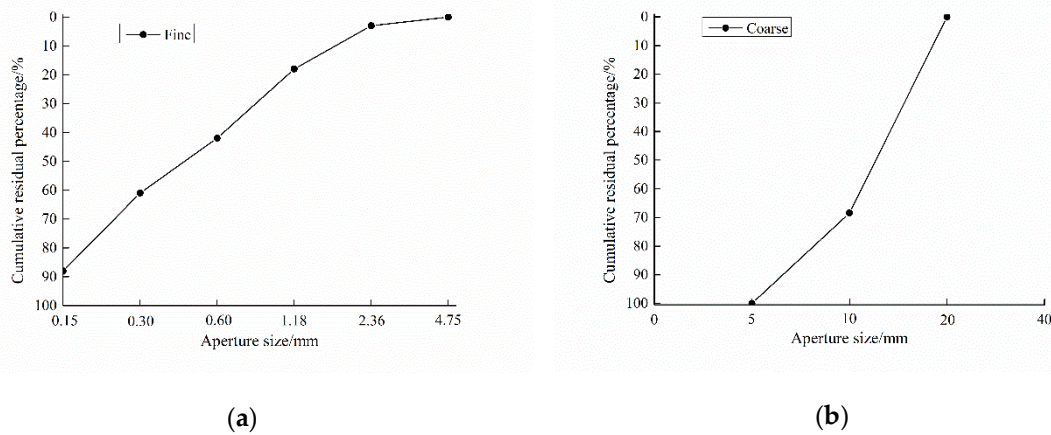


Figure 3. The grain size curve of aggregates: (a) fine; (b) coarse.

Table 4. Mix design of concretes (kg/m<sup>3</sup>).

No.	SO <sub>3</sub> by Weight of Aggregate/%	Cement	Water	Fine Aggregate		Coarse Aggregate	
				River Sand	Gypsum Sand	Limestone	Gypsum Stone
R0	0	420	189	735	0	1110	0
G0.5	0.5					1058	52
G1	1					1006	104
G1.5	1.5					954	156
G3	3	420	189	735	0	798	312
G5	5					590	520
G7	7					382	728
FG0.5	0.5			683	52		
FG1	1			631	104		
FG1.5	1.5			579	156		
FG3	3	420	189	423	312	1110	0
FG5	5			215	520		
FG7	7			7	728		

## 4. Methods

### 4.1. Expansion Test on Concrete

An expansion test was conducted using three specimens per mix. The reference points used to measure the dimensional variations of samples were placed on the 75 mm by 280 mm sides that were in contact with the lateral sides of the molds. As shown in Figure 4, two reference points were placed on each side with 250 mm separation. According to Equation (1), the expansion of a specimen at a certain age was calculated by the average of the measurements performed at both sides with a handholding strain gauge with 0.01% precision. In the formula, *L*<sub>0</sub>, *L*, and *L*<sub>*t*</sub> represent the initial length, effective length of 250 mm, and testing length at different ages, respectively.

$$P = \frac{L_t - L_0}{L} \times 100\% \tag{1}$$



**Figure 4.** Expansion test on concrete.

#### 4.2. Compressive Strength of Concrete

The compressive strength of the concrete cubic specimen was examined at the ages of 28, 60, 90, 150, 210, and 240 days by using a compressive-testing machine with a loading rate 0.5–0.8 MPa/s. The machine for testing compressive strength is shown in Figure 5. For each test, the average compressive strength of the three cubic concrete samples was used.



**Figure 5.** Compressive strength test on cubic concrete.

#### 4.3. Ultrasonic Test on Prism Concrete

The ultrasonic velocities, which describe the material internal damage, in specimens at different ages were tested, by fixing the launcher and receiver transducer firmly on the two sides of the specimen (75 mm by 75 mm), in accordance with the “Technical specification for inspection of concrete defects by ultrasonic method” (CECS 21: 2000). The machine used to test the ultrasonic pulse velocity is shown in Figure 6.



**Figure 6.** Ultrasonic pulse velocity test on prism concrete.

#### 4.4. XRD and Thermogravimetry–Differential Scanning Calorimetry (TG–DSC) Analysis on Mortar

To get the complementary mineral information, mortar specimens were subjected to XRD and TG–DSC analyses at different ages. The mortars cut from the concrete samples were immersed in absolute ethyl alcohol for 12 h to terminate hydration, before being vacuum dried at 60 °C for 24 h, and then ground into powder. The test powders were passed through an 0.08 mm sieve. The XRD data were collected in the range of 10°–70°, 2 $\theta$  at a counting time of 15 s/step, and a divergence slit of 1°. TG–DSC data were obtained from 50 to 950 °C at a rate of temperature increase of 10 °C/min in a N<sub>2</sub> atmosphere.

#### 4.5. Microstructure Examination on Concrete

In order to investigate the morphology of concrete under internal sulfate attack, a fractured fresh piece of concrete was sampled, hydration terminated, and vacuum dried. Then, the dried sample was embedded in a low-modulus epoxy, polished using progressively smaller grids, coated with a gold-palladium coating, and investigated using JSM-7600F SEM.

#### 4.6. Dissolution of WP in Concrete

The pore solution in concrete was expressed directly with a compressive-testing machine whose final pressure value was 2000 MPa at a speed of 2 MPa/s. Then, the sulfate concentration in this pore solution was tested by inductive coupled plasma emission spectrometer (ICP).

## 5. Results

### 5.1. Expansion Measurements

Figure 7a presents the expansion data for the concretes with different amounts of gypsum-contaminated fine aggregate. Figure 7b shows the change in length of concrete with different amounts of contaminated coarse aggregate. The results for the gypsum-contaminated fine aggregate samples show that the mixes with a gypsum content above 3% SO<sub>3</sub> presented a significant increase in expansion for 360 days. There was a little expansion when the SO<sub>3</sub> content in sand was 1.5%, and the expansions of the specimen was less than 0.1% in 360 days. Meanwhile, specimens containing SO<sub>3</sub> less than 1.5% showed no expansion.

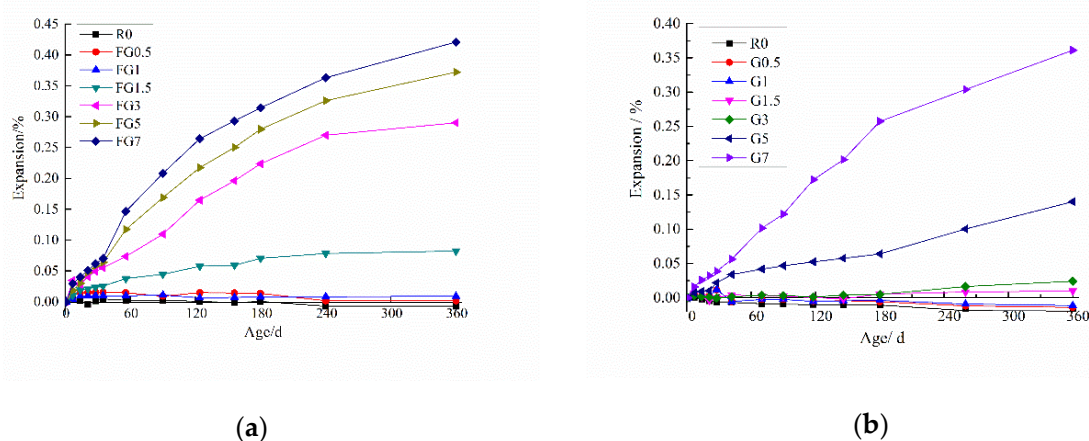


**Figure 7.** Expansion curves of concrete with gypsum-contaminated aggregate: (a) gypsum-contaminated fine aggregate; (b) gypsum-contaminated coarse aggregate.

For the samples with gypsum-contaminated coarse aggregate, no significant variation was observed, when the SO<sub>3</sub> content in coarse aggregate was less than 3%. The average expansion increased obviously as the SO<sub>3</sub> content increased to 5% and 7%. The final measured expansions for the specimens

containing 5% and 7%  $\text{SO}_3$  were 0.1401% and 0.3602%, respectively, at 360 days. The expansion data in Figure 7a indicated that the smaller aggregate particle size resulted in higher expansion of the specimen, at the same  $\text{SO}_3$  content.

Several studies recommended 0.1% expansion as a safe margin for determining the maximum percentage of sulphate than can be present in a mixture without causing any significant degradation [2]. Based on the results shown in Figure 7, FG1.5, FG1, FG0.5, G3, G1.5, G1, and G0.5 comply with the maximum expansion suggested in the literature. Consequently, these mixtures should not show a risk of damage from a structural point of view, but these  $\text{SO}_3$  contents are bigger than the limit established in several standards, such as GB/T14684 and GB/T14685 in China.

### 5.2. Compressive Strength

Figure 8 shows the compressive strength development for concrete with various amounts of gypsum-contaminated aggregate. The results indicate that all concrete specimens exhibited a reduction in initial compressive strength as  $\text{SO}_3$  increased. It was evident that with 0.5–1.5%  $\text{SO}_3$  in sand, the initial compressive strength of concrete decreased by 25%. Additionally, 3–7%  $\text{SO}_3$  in sand led to a loss in the initial compressive strength of samples of about 38%. The compressive strength of all specimens with gypsum-contaminated aggregate increased first and then decreased with the curing age. As shown in Figure 8a, the final strengths of the FG0.5, FG1.0, and FG1.5 specimens at 360 days were higher than the initial strength of the reference sample, which means that an  $\text{SO}_3$  content in sand of less than 1.5% is relatively safe.

For the samples with  $\text{SO}_3$  in coarse aggregate, only the strength of the G7 specimen increased—from 30.2 to 33.3 MPa in 28 days—before reducing to 14.2 MPa at 360 days because of the expansion properties shown in Figure 7. The strength curve of the G5 sample showed a significant decrease after 210 days. It was indicated that samples with gypsum incorporated (0.5–3%  $\text{SO}_3$ ) had less effect on the compressive strength of concrete relative to the initial strength of the reference.

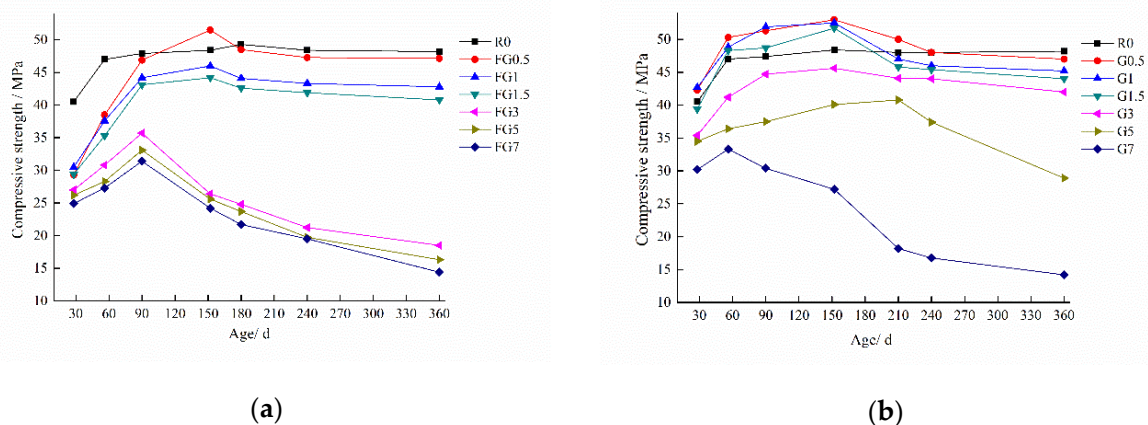


**Figure 8.** Compressive strength of concrete with gypsum-contaminated aggregate: (a) gypsum-contaminated fine aggregate; (b) gypsum-contaminated coarse aggregate.

### 5.3. Ultrasonic Test

The internal damage of specimens under internal sulfate attack was tested by ultrasonic pulse velocity, and the results are presented in Figure 9. The value of ultrasonic velocity is closely related to the microstructure. The more compact a structure is, the higher the ultrasonic velocity obtained will be. The results show that the change trend for the ultrasonic velocities of samples is consistent with that of compressive strength. Except for the FG3, FG5, FG7, G5, and G7 specimens, the damage to the other samples was small.

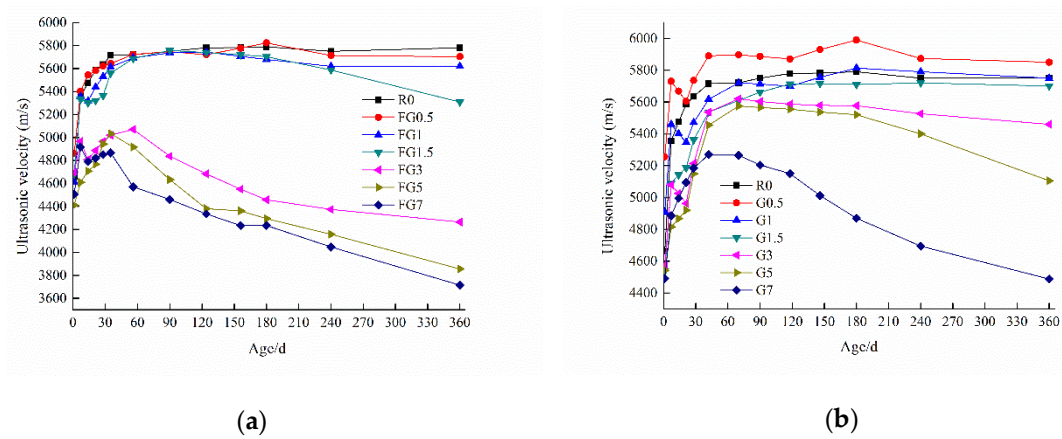


**Figure 9.** Ultrasonic test results of concrete samples: (a) gypsum-contaminated fine aggregate; (b) gypsum-contaminated coarse aggregate.

5.4. Mineral Composition Examination

To detect the existence of gypsum in mortar during the internal sulfate attack, while avoiding the effects of quartz and dolomite peaks in the XRD, the XRD results from 5° to 20° are shown in Figures 10 and 11, for the most intensive peak of gypsum within 20° in the XRD patterns.

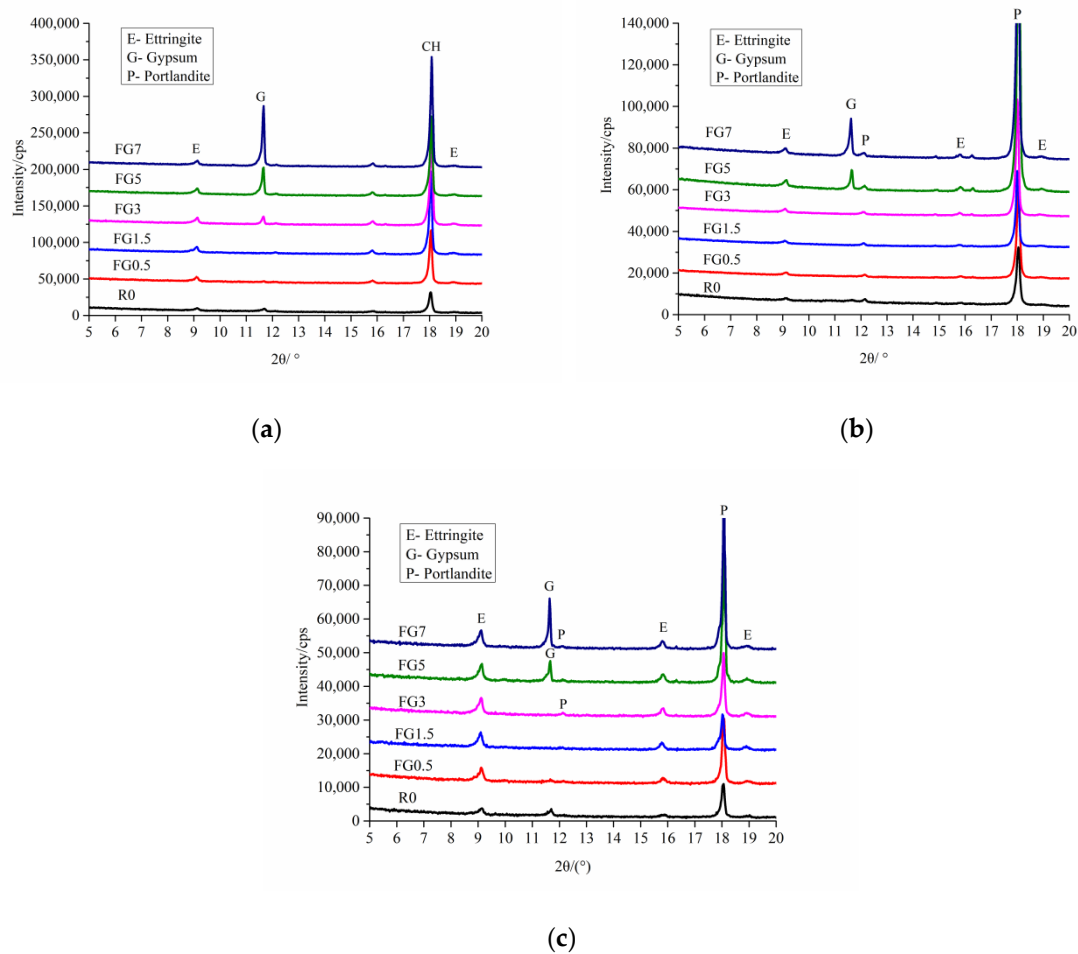


**Figure 10.** XRD patterns of paste in concrete with gypsum-contaminated fine aggregate of different ages: (a) 56 days; (b) 240 days; and (c) 360 days.

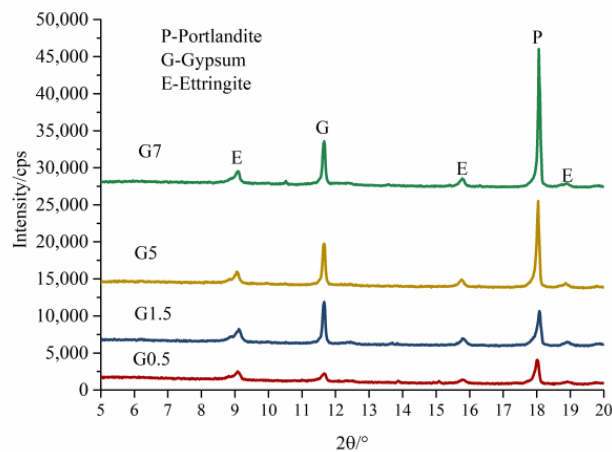


**Figure 11.** XRD patterns of paste in concrete with gypsum-contaminated coarse aggregate at 360 days.

Figure 10 shows a comparison of the X-ray diffractograms of concrete samples with different amounts of  $\text{SO}_3$  in sand at 56, 240, and 360 days. The peaks of ettringite (E), portlandite (P), and gypsum (G) are highlighted in the graph. The results indicate that the mortar in concrete had no gypsum when the  $\text{SO}_3$  content in the sand was less than 1.5% at 56 days. Note that there were apparently no peaks corresponding to gypsum in the FG3 specimen at 240 days. Moreover, for the FG5 and FG7 samples, there was also a certain amount of gypsum in mortar until 360 days. It was clear that during the process of ISA, the gypsum in concrete could be dissolved.

Figure 11 represents the X-ray patterns of concrete containing  $\text{SO}_3$  in coarse aggregate at 360 days. It is worth mentioning that all concrete with gypsum coarse aggregate incorporated had gypsum for 360 days during the internal sulfate attack. This provides evidence that the dissolution rate of gypsum in gypsum-contaminated aggregate with bigger particle size is relatively slower.

The XRD results show that, during ISA the gypsum dissolved when the  $\text{SO}_3$  content was less than 3% in sand. For the higher contents of  $\text{SO}_3$  in FG5 and FG7, the new gypsum phase would be formed by the dissolution of  $\text{SO}_3$ . To solve these problems, the TG–DSC analysis of FG7 specimen was researched. Figure 12 shows the TG–DSC curves of the FG7 samples at ages of 56, 120, and 240 days. As shown in Figure 12b, the temperatures of 80–120, 120–150, and 390–470 °C correspond to the decomposition of AFt ( $3\text{CaO}\cdot\text{Al}_2\text{O}_3\cdot 3\text{CaSO}_4\cdot 32\text{H}_2\text{O}$ ), gypsum ( $\text{CaSO}_4\cdot 2\text{H}_2\text{O}$ ), and portlandite ( $\text{Ca}(\text{OH})_2$ ), respectively. During heating from 80 to 120 °C, 26 mol of water will be removed from AFt [18]. The amount of AFt in the specimen can be calculated by Equation (2). According to the mass loss (at 120–150 °C and 390–470 °C) caused by the decomposition of  $\text{CaSO}_4\cdot 2\text{H}_2\text{O}$  and  $\text{Ca}(\text{OH})_2$  (shown in Figure 12a), the quantities of gypsum and portlandite can be calculated using Equation (3) and Equation (4).

$$\text{AFt}(\%) = W_{\text{AFt}} \cdot \frac{M_{\text{AFt}}}{26M_{\text{H}}} \quad (2)$$

$$\text{G}(\%) = W_{\text{G}} \cdot \frac{M_{\text{G}}}{2M_{\text{H}}} \quad (3)$$

$$\text{P}(\%) = W_{\text{P}} \cdot \frac{M_{\text{P}}}{2M_{\text{H}}} \quad (4)$$

where  $W_{\text{AFt}}$ ,  $W_{\text{G}}$ , and  $W_{\text{P}}$  correspond to the mass loss in percentage attributable to AFt, gypsum, and portlandite dehydration, respectively, and  $M_{\text{AFt}}$ ,  $M_{\text{G}}$ , and  $M_{\text{P}}$  are the molecular weights of AFt, gypsum, and portlandite, respectively.  $M_{\text{H}}$  is the molecular weight of  $\text{H}_2\text{O}$ .

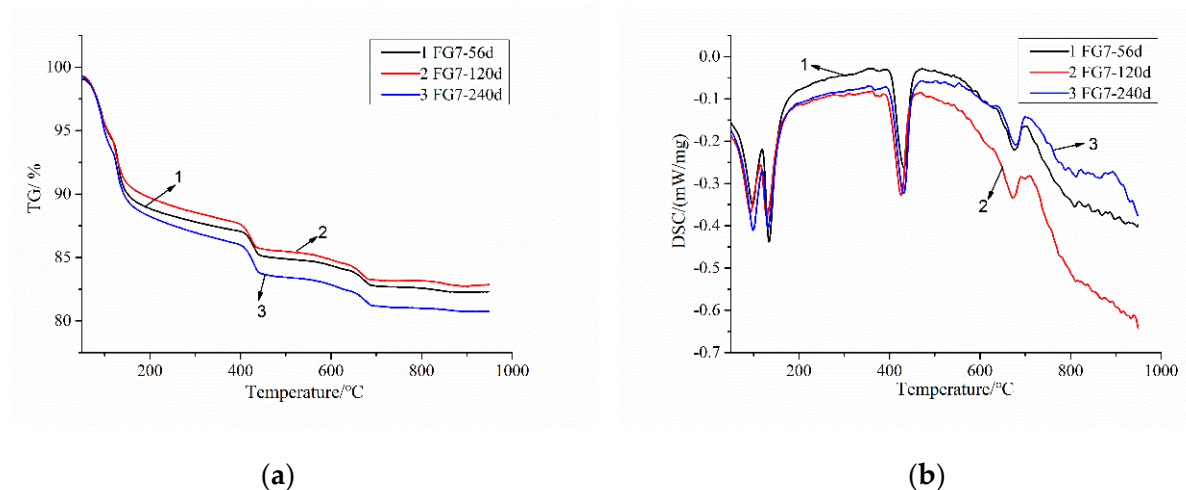


**Figure 12.** Thermogravimetry–differential scanning calorimetry (TG–DSC) curves of the FG7 specimen at the ages of 56, 120, and 240 days. (a) TG; (b) DSC.

Figure 13 shows the estimated quantities of AFt and gypsum at 56, 120, and 240 days. The results show that the amount of gypsum phase decreased and the quantity of AFt increased during the ISA. Additionally, the amount of portlandite stayed relative stable throughout the whole process.

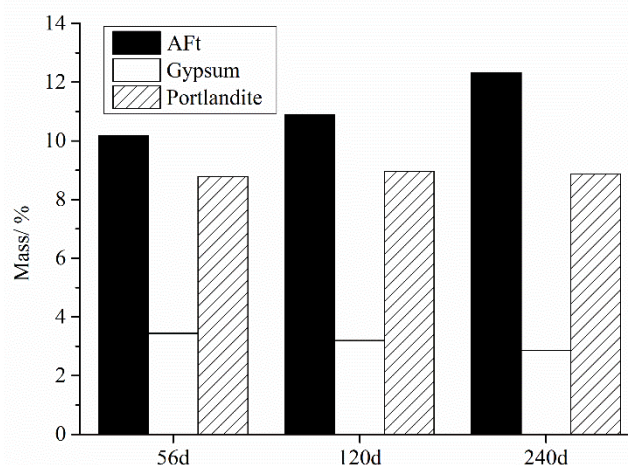


**Figure 13.** Estimated quantities of ettringite (AFt) and gypsum at 56, 120, and 240 days in concrete.

### 5.5. WP Dissolution in Concrete

Figure 14 shows the concentration of  $\text{SO}_4^{2-}$  in the pore solution in concrete at different ages. As shown in Figure 14, concrete with 5% and 7%  $\text{SO}_3$  in aggregate showed a higher concentration of sulfate ions as compared to the reference sample at all ages. The sulfate concentration increased with an increase in the gypsum content in specimens. Figure 14 also indicates that the  $\text{SO}_4^{2-}$  dissolved more easily for aggregate with a smaller particle size, which is consistent with the results for the expansion and compressive strength of samples. Furthermore, for the FG7 specimen, the concentration of  $\text{SO}_4^{2-}$  was 0.0408 mol/L, which exceeded the minimum concentration of sulfate ions (1400 mg/L) to form gypsum in solution [11]. However, this number is much smaller than 8000 mg/L, the sulfate ion concentration required for external sulfate attack to form gypsum [12]. Additionally, as the mineral analysis results showed that portlandite did not decrease, this means that there was no new phase of gypsum formed.

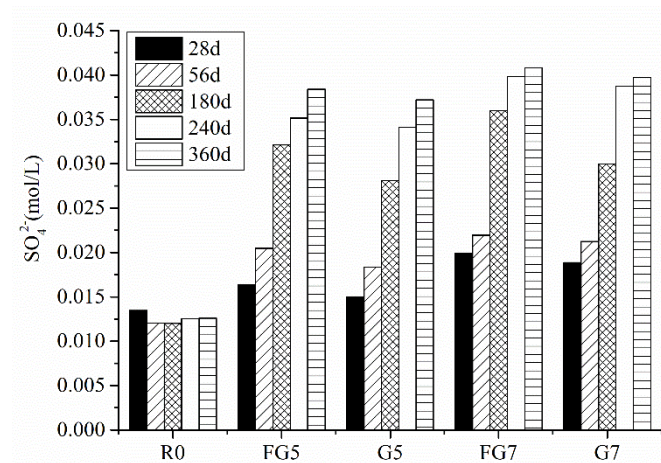


Figure 14. Concentration of SO<sub>4</sub><sup>2-</sup> in the pore solution at different ages.

5.6. Microstructure

SEM was applied to observe the microstructure of mortar with 5% SO<sub>3</sub> in sand. Figure 15 shows the cracking behavior of concrete with 5% SO<sub>3</sub> in sand at 120 and 240 days. It is shown that with the development of ISA, the fracture firstly extended from the gypsum to the paste. Then, the crack extended around the sand, and finally, the sand separated from the paste completely. Figure 16 shows the crack width change during the ISA. The picture shows that the crack width increased significantly. Additionally, in the crack, the needle ettringite crystals oriented their growth in the surface between the paste and aggregate, as shown in Figure 17. Thus, the formation of ettringite was the cause of ISA in the concrete with gypsum-contaminated aggregate.

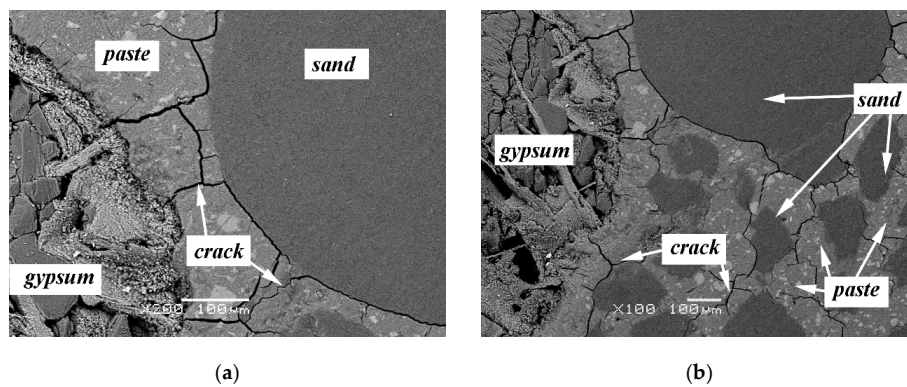


Figure 15. SEM photographs of cracking behavior of concrete with 5% SO<sub>3</sub> in sand: (a) 120 days; (b) 240 days.

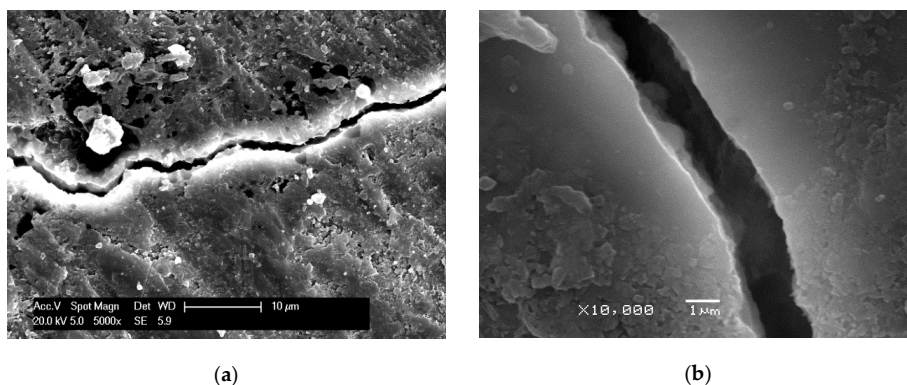
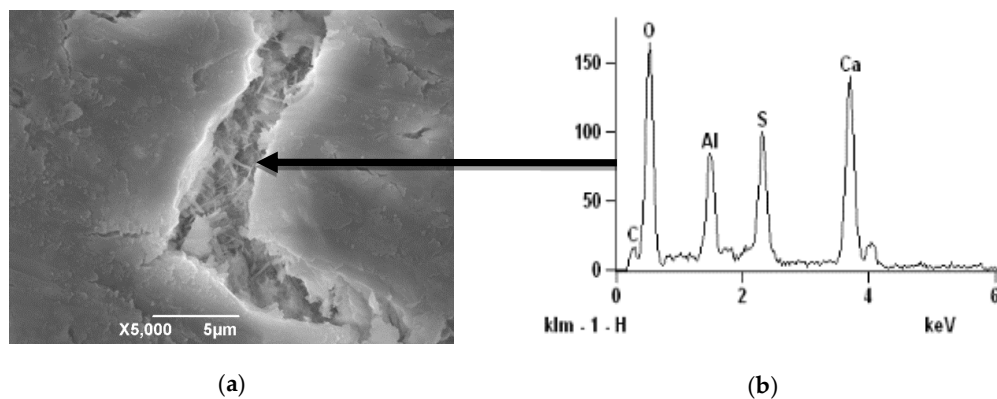


Figure 16. SEM photographs of crack width in concrete: (a) 120 days; (b) 240 days.



**Figure 17.** SEM images of cracking and EDS image of product in crack. (a) SEM; (b) EDS.

## 6. Conclusions

The deterioration process of concrete exposed to internal sulfate attack was investigated. The main conclusions are as follows:

- With an increase in the  $\text{SO}_3$  content in aggregate, the concrete expansion increased, and the compressive strength decreased. However, if the  $\text{SO}_3$  content was lower than 1.5% and 3% in fine aggregate and coarse aggregate, respectively. Although, the expansion was not obvious, and the compressive strength of samples was above the initial strength of the reference specimen. The critical values of  $\text{SO}_3$  content in fine and coarse aggregate were found to be 1.25% and 3%, respectively. At values above these harmful expansion and large strength loss appear.
- $\text{SO}_4^{2-}$  dissolved more easily when the particle size of aggregate was smaller. When the  $\text{SO}_3$  content in the sand was less than 1.5% at 56 days, all the gypsum was dissolved. That was the reason why the expansion of specimens with a smaller  $\text{SO}_3$  content (1.25% for fine aggregate and 3% for coarse aggregate) was not significant.
- The concentration of sulfate ions in the pore solution of concrete was not enough to form a new phase of gypsum when the  $\text{SO}_3$  content was less than 7% in aggregate. For the internal sulfate attack, the main reaction product is ettringite, which causes the expansion of specimens.
- The fracture mode of internal sulfate attack was the crack extending from gypsum particles to paste, which made the aggregate separate from the paste.
- In this paper, only TG–DSC was used to analyze the content of major phases, and no other methods were combined. This paper only studied the changes in compressive strength and expansion performance of concrete containing gypsum aggregates for 360 days. To study whether it is safe to use gypsum aggregates in concrete, other durability tests are needed. In addition, there has been lack of evaluation on methods that can be used to determine the safe dosage of gypsum aggregate in concrete at home and abroad, which will be the focus of our follow-up work.

**Author Contributions:** Conceptualization, W.C. and B.H.; data curation, W.C. B.H. and Y.Y.; writing—original draft preparation, W.C.; writing—review and editing, B.H. and M.D. All authors have read and agreed to the published version of the manuscript.

**Funding:** This research was funded by National Natural Science Foundation of China 51608265, and Anhui Key Laboratory of Advanced Construction Materials at Anhui Jianzhu University JZCL 200604KF.

**Acknowledgments:** The authors gratefully acknowledge the assistance from Zhongyang Mao, Huan Yuan, Jun Wang from NJTECH, and the staff from State Key Laboratory of Materials-Oriented Chemical Engineering.

**Conflicts of Interest:** The authors declare no conflict of interest.

## References

1. Hime, W.G.; Mather, B. "Sulfate attack," or is it. *Cem. Concr. Res.* **1999**, *29*, 789–791. [[CrossRef](#)]
2. Skalny, J.; Marchand, J.; Odler, I. *Sulfate Attack on Concrete*; Spon Press: London, UK, 2002.
3. Leemann, A.; Löser, R. Analysis of concrete in a vertical ventilation shaft exposed to sulfate-containing groundwater for 45 years. *Cem. Concr. Compos.* **2011**, *33*, 74–83. [[CrossRef](#)]
4. Ma, B.; Gao, X.; Byars, E.A.; Zhou, Q. Thaumaside formation in a tunnel of Bapanxia Dam in Western China. *Cem. Concr. Res.* **2006**, *36*, 716–722. [[CrossRef](#)]
5. Gesoglu, M.; Guneyisi, E.; Nahhab, A.H.; Yazıcı, H. The effect of aggregates with high gypsum content on the performance of ultra-high strength concretes and Portland cement mortars. *Constr. Build. Mater.* **2016**, *110*, 346–354. [[CrossRef](#)]
6. Crammond, N. The thaumasite form of sulfate attack in the UK. *Cem. Concr. Compos.* **2003**, *25*, 809–818. [[CrossRef](#)]
7. Janković, K.; Miličić, L.; Stanković, S.; Šušić, N. Investigation of the mortar and concrete resistance in aggressive solutions. *Tehnički Vjesnik* **2014**, *21*, 173–176.
8. Fu, Y.; Gu, P.; Xie, P.; Beaudoin, J. A kinetic study of delayed ettringite formation in hydrated portland cement paste. *Cem. Concr. Res.* **1995**, *25*, 63–70. [[CrossRef](#)]
9. Clark, B.A.; Brown, P.W. The formation of ettringite from tricalcium aluminate and magnesium sulphate. *Adv. Cem. Res.* **2000**, *12*, 137–142. [[CrossRef](#)]
10. Tian, B.; Cohen, M.D. Expansion of Alite Paste Caused by Gypsum Formation during Sulfate Attack. *J. Mater. Civ. Eng.* **2000**, *12*, 24–25. [[CrossRef](#)]
11. Bellmann, F.; Moser, B.; Stark, J. Influence of sulfate solution concentration on the formation of gypsum in sulfate resistance test specimen. *Cem. Concr. Res.* **2006**, *36*, 358–363. [[CrossRef](#)]
12. Santhanam, M.; Cohen, M.D.; Olek, J. Sulfate attack research—Whither now? *Cem. Concr. Res.* **2001**, *31*, 845–851. [[CrossRef](#)]
13. Scholtzová, E.; Kucková, L.; Kožíšek, J.; Palkova, H.; Tunega, D. Experimental and computational study of thaumasite structure. *Cem. Concr. Res.* **2014**, *59*, 66–72. [[CrossRef](#)]
14. Kohler, S.; Heinz, D.; Urbonas, L. Effect of ettringite on thaumasite formation. *Cem. Concr. Res.* **2006**, *36*, 697–706. [[CrossRef](#)]
15. Oliveira, I.; Cavalaro, S.H.P.; Aguado, A. New kinetic model to quantify the internal sulfate attack in concrete. *Cem. Concr. Res.* **2013**, *43*, 95–104. [[CrossRef](#)]
16. Samarai, M.A. The disintegration of concrete containing sulphate-contaminated aggregates. *Mag. Concr. Res.* **1976**, *28*, 130–142. [[CrossRef](#)]
17. Crammond, N. Examination of mortar bars containing varying percentages of coarsely crystalline gypsum as aggregate. *Cem. Concr. Res.* **1984**, *14*, 225–230. [[CrossRef](#)]
18. Qoku, E.; Bier, T.; Westphal, T. Phase assemblage in ettringite-forming cement pastes: A X-ray diffraction and thermal analysis characterization. *J. Build. Eng.* **2017**, *12*, 37–50. [[CrossRef](#)]

